Characterization of the Displacement Tolerance of QCA Interconnects

Faizal Karim, *Student Member, IEEE* and Konrad Walus, *Member, IEEE,*

***Abstract*— Quantum-Dot Cellular Automata (QCA) is one of several emerging nanoscale devices that is targeted at scalable molecular electronics. In this paper, the tolerance to cell displacements of a QCA interconnect is analysed in order to determine limits on allowable displacements, as well as to identify the important failure mechanisms. Numerical simulations using the coherence vector formalism are performed for a short length of QCA interconnect under various conditions. Contrary to previous work, our results indicate that wider interconnects display a higher sensitivity to cell displacements due to the formation of cell clusters, which are more prominent in wider interconnects as a result of the increased number of cells.**

I. Introduction

Molecular quantum-dot cellular automata (QCA) has been proposed by Lent *et al*. [1], [2] as a scalable implementation of molecular electronics for computing. Although several experimental results have been reported [3]–[6], work is still underway to determine the exact structure of such molecules. QCA breaks from the standard route of mimicking transistor action at the nanoscale and instead uses the electronic configurations of the molecular system to encode and process binary information. With this approach, no physical connection is required to individual molecules [2], [7], [8], making molecular QCA a more appropriate approach to computing using molecules. Using QCA, significant research has been reported on circuit design [9]–[14] and testing [15]–[17]. Fabrication of such devices however, remains a primary hurdle for this computing paradigm. In an effort to ease the fabrication process and provide more tolerance to potential fabrication defects, the use of n-cell wide interconnects has generated considerable interest in recent years [17]–[21]. It is assumed that the increased interconnect width introduces an additional level of redundancy which contributes to the interconnect's ability to withstand cellular defects, including random cell displacements. However, while earlier work has analysed the effect of cell displacements on various building blocks including the interconnect [17]–[23], it has not fully explained the important parameters on interconnect displacement tolerance, nor has it investigated the effect of increased interconnect width. It is shown in this work that increasing the width of interconnects does not provide any more tolerance to these cellular displacements.

This work was supported, in part, by research grants from the Natural Sciences and Engineering Research Council of Canada

F. Karim and K. Walus are with the Microsystems and Nanotechnology Research Group at the University of British Columbia, Department of Electrical and Computer Engineering, 2332 Main Mall, Vancouver, BC, Canada V6T 1Z4 Phone: 604-827-3412, Fax: 604-822-5949 (e-mail: {faizalk,konradw}@ece.ubc.ca).

II. Description of Numerical Simulations

All simulations were performed using the QCADesigner tool [24] using a simulation engine that models the cells and circuits using the coherence vector formalism described in [25], [26]. Simulations were executed on a high-performance computer cluster consisting of 174 Intel Xeon CPU cores on 32 nodes, each with memory ranging from 8 to 16GB, although most simulations used a small fraction of the available RAM. In total over 10,000 simulations were performed, each lasting approximately 2.5 hours.

The displacement of each cell in the simulated circuits was represented by a random variable, X, characterized by a Gaussian distribution with a mean value equal to the original location of the cell and a standard deviation, σ. Each cell is displaced without rotation. For each data point, 500 unique simulations are performed for a single value of σ using a batch simulation mode in QCADesigner, and the percentage of circuits that successfully complete the simulation is recorded. Cell size (dot-dot distance) is chosen to be 1nm and cell spacing is chosen to be twice the dot-dot distance. Note that the cell size definition differs by a factor of 2 from previous work [22]. The dielectric constant for all simulations is chosen to be, ϵ_r=1, consistant with a molecular implementation.

Simulation parameters were scaled according to the interaction energy (kink energy) between neigboring cells. The relaxation time, τ, is chosen to be $\tau = 5\hbar/E_{\text{kink}}$, time step is $\Delta t = \tau/1500$ and the simulation duration is $T = 1000\tau$. The time step was set to three orders of magnitude smaller than the relaxation time in order to prevent divergence during our simulations. The simulation temperature was chosen to be 1 K for all simulations. The standard deviation of the cell displacements, σ, was chosen to range from 0 to 100% of the cell size (dot-dot distance). The maximum tunneling energy was $\gamma_{\text{max}} = 2E_{\text{kink}}$ and the minimum was $\gamma_{\text{min}} = 0.3E_{\text{kink}}$. The simulation engine parameters (the time step and the relaxation time) are further explained in [22]. We gauge the successful operation of each circuit by comparing the simulation output of the randomly modified circuit with the simulation output of a reference circuit that we have previously verified to be logically correct. Input vectors for all simulations were the same, input = 0101100. Circuits that were more than one cell wide had multiple input cells, each of which was presented with the same input value. The output waveforms were not themselves compared. Instead, output waveforms were interpreted using a simple threshold system: polarization $<$ lower threshold (usually -0.5) logic 0 and polarization $>$ upper threshold (usually 0.5) logic 1, otherwise the state is indeterminate. The logical output of the circuit is then

compared versus the known working circuit output pattern.

III. Results

A. Clock Electrode Spacing

Hennessy *et al*. have shown that it is possible to clock a molecular QCA circuit using submerged electrodes [2]. These electrodes produce a near vertical forward traveling electric field at the level of cells as shown in Fig. 1. Here, the signal applied to each of the four electrodes shown in Fig. 1 is shifted by ϕ_i as indicated on the electrodes, such that $\phi_1 < \phi_2 < \phi_3 < \phi_4$. When the applied electric field on the cell in the $\hat{y}$ direction, $\vec{E_y}$, is sufficiently large, it will draw the mobile electrons towards the bottom two sites of the cell forcing the cell into the "null" state. Conversely, if the electric field on the electrodes becomes strongly negative, it will drive the electrons to the upper sites of the cell and force it into one of the "active" states. If the field is only somewhat positive or negative, the cell will be in a switching state, occupying the upper sites of the cell but still allowed to tunnel through the lower sites and switch its configuration.

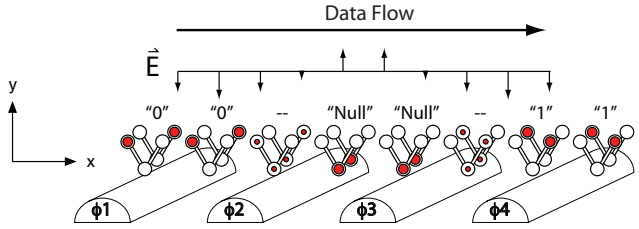

Fig. 1. Submerged electrodes can be used to clock QCA cells by generating a forward moving electric field at the level of the cells. A ground plane located above the cells is not shown in the figure. The sizing of the QCA cells are not to scale with respect to the spacing of the electrodes, and many cells can be placed between adjacent electrodes.

Computation is performed at the wavefront of this forward moving wave, where cells are switched from the null to active states. The number of cells in the active region is a function of the electrode spacing, the total number of phases over which the electrodes are divided, and the range of applied potential. Assuming that each electrode is excited by a sinusoid with phase difference of $\pi/2$; *i.e.*, a 4 phase clock, the wavenumber of the clocking wave, k, can be calculated using, $k = \frac{\pi}{2s}$, where, s is the inter-electrode spacing. For low wavenumbers; *i.e.*, spatial waves with long wavelengths, many cells are in the switching state, and many cells are in the active state. Within the current version of the QCADesigner tool, each cell is assigned a particular clock signal and relative phase. The clock is implemented in the tool by direct modulation of the tunneling barriers between sites of a two-state cell while the approach proposed by Hennessy *et al.* is based on a three-state cell. It is believed that for an appropriate choice of clocking parameters and assuming the system evolves adiabatically, the tolerance to displacements is determined entirely by geometric and interaction energy considerations rather than a result of cell dynamics. To this end, the results presented here attempt to approximate the full solution of the continuous wave clocking approach by modifying the relative phase of the clock signal applied to neighboring cells.

Semi-classical analysis has shown that longer interconnects are more susceptible to thermal fluctuations resulting in error [27], indicating that shorter interconnects or smaller active regions are preferable. Earlier work on displacements were performed using a wavenumber of 0, *i.e.*, all cells switched simultaneously [22]. However, it was not clear if the size of the active region has any effect on the tolerance to cell displacements. The phase difference in clock signal experienced by neighboring cells with 4 phase clocking is given by,

$$\phi_{cc} = \frac{\pi}{2(n-1)}, \tag{1}$$

where n is the number of cells between and above two electrodes. By adjusting this relative phase, various clock wavenumbers are simulated. Simulations were performed for circuits with relative phases of $30°, 25°, 20°, 15°, 10°, 5°$, and $0°$, which is equivalent to placing 4, 5.5, 10, 19, and ∞ cells in between adjacent clocking electrodes. Fig. 2 shows the results of these simulations.

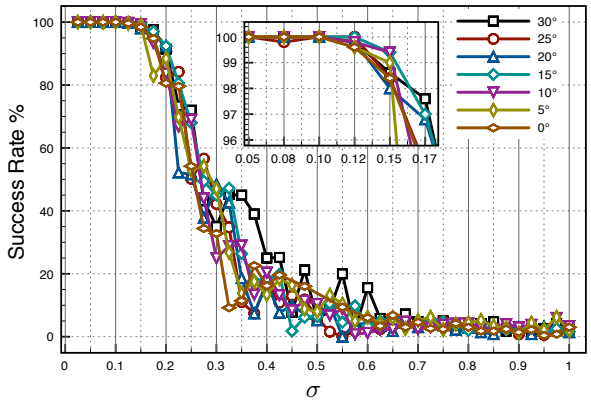

Fig. 2. Success rate for interconnect of single cell width for decreasing clock phase between cells.

It is clear from these results, that the spacing between electrodes, and hence the size of the active region, has no noticable effect on the tolerance of QCA interconnects to displacements.

B. Interconnect Width

Simulations were performed on interconnects of increasing width (shown in Fig. 3). It was expected that increasing the width of the interconnect would increase the ability for the interconnect to absorb faults, and hence increase the displacement tolerance. To determine the effect of interconnect width, simulations were performed with interconnect width increasing from 1 to 6 cells. Results of these simulations are shown in Fig. 4. Fig. 4 shows that there is a threshold value, $\sigma \approx 0.12$ nm, before which the probability of success of each interconnect is 100%. While this threshold value is common to all interconnects, the decrease in success rate

as a function of σ is different for each interconnect, with wider interconnects displaying a higher sensitivity to cell displacements. This effect is believed to result from the larger number of possible configurations in which an error has occurred. While it is likely that such wide interconnects can absorb single cell displacements, the same does not appear to be true for interconnects in which all cells can have some displacements.

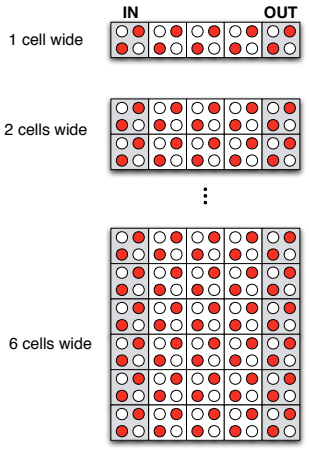

Fig. 3. Interconnects of various widths.

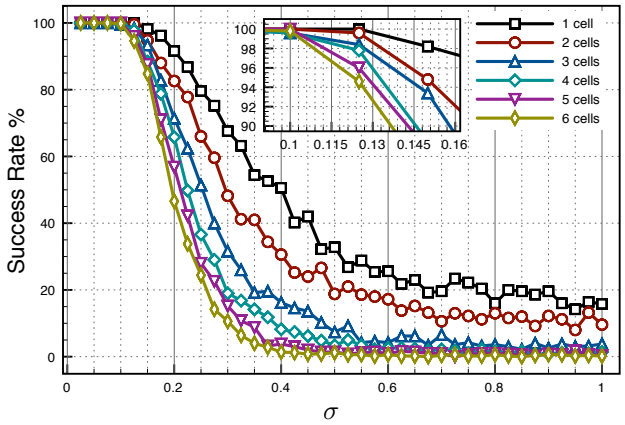

Fig. 4. Success rate for interconnect of increasing width.

C. Number of Displaced Cells

Previous simulations were performed by displacing *all* cells in an interconnect. Here, we consider an interconnect's ability to absorb faults as the number of displaced cells is increased. In a first simulation, an interconnect with a width of 6 cells was considered, with the number of displaced cells ranging from 3 to 18 cells (input and output cells were not displaced). The results of this simulation are shown in Fig. 5. As expected, as the number of displaced cells increases, so does the rate at which the interconnect fails. However, Fig. 5 also shows that in spite of its width, the threshold value of σ for the 6-cell wide interconnect before which the probability of success of each interconnect is 100%, is approximately 0.13 nm. It will be shown in a following simulation that this σ value increases for thinner interconnects.

TABLE I
SUCCESS RATES FOR INTERCONNECTS OF DIFFERENT WIDTHS

Displaced Cells	Interconnect Width					
	1	2	3	4	5	6
3	29.60%	29.20%	31.20%	24.20%	24.40%	20.00%
6	-	16.80%	11.20%	8.60%	8.80%	8.20%
9	-	-	6.20%	5.40%	5.20%	2.00%
12	-	-	-	3.60%	3.20%	0.80%
15	-	-	-	-	2.40%	0.60%
18	-	-	-	-	-	0.60%

Table 1 shows a comparison of the success rates for all 6 considered interconnects as the number of displaced cells is varied. σ was kept constant at 1.00. The results shown in Table 1 indicate that wider interconnects do not provide any more capacity for absorbing displacement faults than do thinner interconnects.

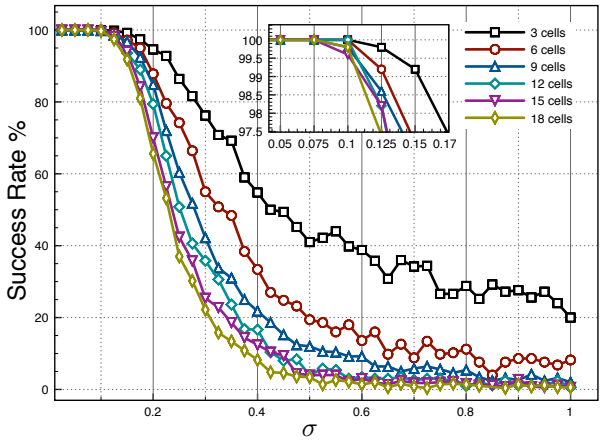

Fig. 5. Success rate for interconnect of 6 cell width for increasing number of displaced cells.

For a second simulation, the success rates of two interconnects with different widths were compared as a percentage of their cells were displaced. The results of this simulation are shown in Fig. 6. Here, a single and 6-cell wide interconnect were compared. Each interconnect was simulated having 33%, 67%, and 100% of its cells displaced. From Fig. 6, we see that the interconnect of single cell width is more tolerant to the cell displacements than the 6-cell wide interconnect. This is likely a result of larger cell clusters forming in the 6-cell wide interconnect due to the increased number of displaced cells.

IV. DISCUSSION

The results in this work contradict what was reported in [18]–[21] which had suggested that wider interconnects would provide more tolerance to random cell displacements. It is believed that the presence of cell clusters is what is causing the interconnects to fail. The interaction energy between the clustered cells increases to a level beyond which the clock is able to turn them off. As a result, these cells relax to the

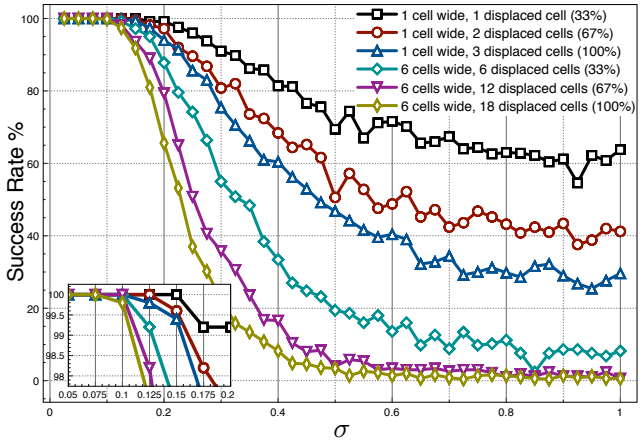

Fig. 6. Success rates for single and 6 cell wide interconnects for increasing number of displaced cells.

polarization provided by the first input in the simulation, and since the clock was unable to fully turn them off, remained in that polarization throughout the rest of the simulation - essentially creating a fixed cell in the middle of the interconnect. If all cells can be displaced, the probability of one of these cell clusters forming is the same for all interconnects irrespective of its width, and hence, wider interconnects do not increase the tolerance to such cell displacements.

V. Conclusions

The tolerance to random cell displacements in a QCA interconnect have been analysed in this paper. It is found that the number of cells between two clocking clocking electrodes does not have an effect on the tolerance of the interconnect to random cell displacements. It was also shown that increasing the width of the interconnect does not contribute to additional displacement tolerance. In fact, it was shown that wider interconnects demonstrated a higher sensitivity to cellular displacements. This result was due to the presence of cell clusters in the interconnect that behave as fixed cells once formed. It was found that these cell clusters were more prominent in wider interconnects due to the increased number of cells.

References

[1] C. S. Lent, "Molecular electronics - bypassing the transistor paradigm," *Science*, vol. 288, no. 5471, pp. 1598–1599, 2000.

[2] K. Hennessy and C. S. Lent, "Clocking of molecular quantum-dot cellular automata," *Journal of Vacuum Science & Technology B*, vol. 19, no. 5, pp. 1752–1755, 2001.

[3] M. Lieberman, S. Chellamma, B. Varughese, Y. L. Wang, C. Lent, G. H. Bernstein, G. Snider, and F. C. Peiris, "Quantum-dot cellular automata at a molecular scale," *Molecular Electronics Ii*, vol. 960, pp. 225–239, 2002.

[4] H. Qi, S. Sharma, Z. H. Li, G. L. Snider, A. O. Orlov, C. S. Lent, and T. P. Fehlner, "Molecular quantum cellular automata cells. electric field driven switching of a silicon surface bound array of vertically oriented two-dot molecular quantum cellular automata," *Journal of the American Chemical Society*, vol. 125, no. 49, pp. 15250–15259, 2003.

[5] W. C. Hu, K. Sarveswaran, M. Lieberman, and G. H. Bernstein, "High-resolution electron beam lithography and dna nano-patterning for molecular qca," *Ieee Transactions on Nanotechnology*, vol. 4, no. 3, pp. 312–316, 2005.

[6] H. Qi, A. Gupta, B. C. Noll, G. L. Snider, Y. H. Lu, C. Lent, and T. P. Fehlner, "Dependence of field switched ordered arrays of dinuclear mixed-valence complexes on the distance between the redox centers and the size of the counterions," *Journal of the American Chemical Society*, vol. 127, no. 43, pp. 15218–15227, 2005.

[7] C. S. Lent and B. Isaksen, "Clocked molecular quantum-dot cellular automata," *IEEE Transactions on Electron Devices*, vol. 50, no. 9, pp. 1890–1896, 2003.

[8] Y. Lu, M. Liu, and C. Lent, "Molecular quantum-dot cellular automata: From molecular structure to circuit dynamics," *Journal of Applied Physics*, vol. 102, no. 3, pp. 034311–7, 2007.

[9] P. D. Tougaw and S. L. Craig, "Logical devices implemented using quantum cellular automata," *Journal of Applied Physics*, vol. 75, no. 3, pp. 1818–1825, 1994.

[10] C. S. Lent and P. D. Tougaw, "Device architecture for computing with quantum dots," *Proceedings of the IEEE*, vol. 85, no. 4, pp. 541–557, 1997.

[11] K. Walus, G. Schulhof, and G. A. Jullien, "High level exploration of quantum-dot cellular automata (qca)," in *Conference Record of the Thirty-Eighth Asilomar Conference on Signals, Systems and Computers*, vol. 1, pp. 30–33 Vol.1, 2004.

[12] K. Walus, G. Schulhof, G. A. Jullien, R. Zhang, and W. Wang, "Circuit design based on majority gates for applications with quantum-dot cellular automata," in *Conference Record of the Thirty-Eighth Asilomar Conference on Signals, Systems and Computers*, vol. 2, pp. 1354–1357 Vol.2, 2004.

[13] R. M. Zhang, K. Walus, W. Wang, and G. A. Jullien, "A method of majority logic reduction for quantum cellular automata," *IEEE Transactions on Nanotechnology*, vol. 3, no. 4, pp. 443–450, 2004.

[14] R. Ravichandran, S. K. Lim, and M. Niemier, "Automatic cell placement for quantum-dot cellular automata," *Integration-the Vlsi Journal*, vol. 38, no. 3, pp. 541–548, 2005.

[15] P. Gupta, N. K. Jha, and L. Lingappan, "Test generation for combinational quantum cellular automata (qca) circuits," 2006. 1131568 311-316.

[16] P. Gupta, N. K. Jha, and L. Lingappan, "A test generation framework for quantum cellular automata circuits," *IEEE Transactions on Very Large Scale Integration (Vlsi) Systems*, vol. 15, no. 1, pp. 24–36, 2007.

[17] M. Khatun, T. Barclay, I. Sturzu, and P. D. Tougaw, "Fault tolerance properties in quantum-dot cellular automata devices," *Journal of Physics D-Applied Physics*, vol. 39, no. 8, pp. 1489–1494, 2006.

[18] M. Khatun, T. Barclay, I. Sturzu, and P. Tougaw, "Fault tolerance calculations for clocked quantum-dot cellular automata devices," *J. App. Phys.*, vol. 98, p. 7, 2005.

[19] A. Finjay and B. N. Toomarian, "New design for quantum dots cellular automata to obtain fault tolerant logic gates," *J. of Nanoparticle Research*, vol. 3, pp. 27–37, 2001.

[20] E. P. Blair, *Tools for the design and simulation of clocked molecular quantum-dot cellular automata circuits*. M.sc., University of Notre Dame, 2003.

[21] E. P. Blair and C. S. Lent, "An architecture for molecular computing using quantum-dot cellular automata," in *3rd IEEE Conference on Nanotechnology*, vol. 1, pp. 402–405 vol.2, 2003.

[22] G. Schulhof, K. Walus, and G. A. Jullien, "Simulation of random cell displacements in QCA," *J. Emerg. Technol. Comput. Syst.*, vol. 3, no. 1, p. 2, 2007.

[23] M. Tahoori, M. Momenzadeh, J. Huang, and F. Lombardi, "Defects and faults in quantum cellular automata at nano scale," in *Proc. of the 22nd IEEE VLSI Test Symposium*, 2004.

[24] K. Walus, T. J. Dysart, G. A. Jullien, and R. A. Budiman, "QCADesigner: a rapid design and simulation tool for quantum-dot cellular automata," *Nanotechnology, IEEE Transactions on*, vol. 3, no. 1, pp. 26–31, 2004.

[25] G. Toth, *Correlation and Coherence in Quantum-Dot Cellular Automata*. Ph.d., University of Notre Dame, 2000.

[26] G. Toth and C. S. Lent, "Role of correlation in the operation of quantum-dot cellular automata," *Journal of Applied Physics*, vol. 89, no. 12, pp. 7943–7953, 2001.

[27] C. Ungarelli, S. Francaviglia, M. Macucci, and G. Iannaccone, "Thermal behavior of quantum cellular automaton wires," *Journal of Applied Physics*, vol. 87, no. 10, pp. 7320–7325, 2000.